HHS Public Access

Author manuscript

Biomaterials. Author manuscript; available in PMC 2017 January 01.

Published in final edited form as:

Biomaterials. 2016 January ; 77: 87–97. doi:10.1016/j.biomaterials.2015.11.005.

Mesenchymal stem cells engineered to express selectin ligands and IL-10 exert enhanced therapeutic efficacy in murine experimental autoimmune encephalomyelitis

Wenbin Liao[a], **Victor Pham**[a,b], **Linan Liu**[a], **Milad Riazifar**[a], **Egest J Pone**[a], **Shirley Xian Zhang**[a], **Fengxia Ma**[a,c], **Mengrou Lu**[a], **Craig M. Walsh**[d], and **Weian Zhao**[a,*]

[a]Department of Pharmaceutical Sciences, Department of Biomedical Engineering, Sue and Bill Gross Stem Cell Research Center, Chao Family Comprehensive Cancer Center & Edwards Lifesciences Center for Advanced Cardiovascular Technology, University of California, Irvine, 845 Health Sciences Road, Irvine, CA 92697, USA

[b]California State University of Fullerton BSCR Program, Fullerton, CA 92831, USA

[c]State Key Laboratory of Experimental Hematology, Institute of Hematology and Blood Disease Hospital, Chinese Academy of Medical Sciences and Peking Union Medical College, Tianjin 300020, China

[d]Department of Molecular Biology and Biochemistry, Sue and Bill Gross Stem Cell Center, Multiple Sclerosis Research Center, University of California, Irvine, Irvine, CA 92697, USA

Abstract

Systemic administration of mesenchymal stem cells (MSCs) affords the potential to ameliorate the symptoms of Multiple Sclerosis (MS) in both preclinical and clinical studies. However, the efficacy of MSC-based therapy for MS likely depends on the number of cells that home to inflamed tissues and on the controlled production of paracrine and immunomodulatory factors. Previously, we reported that engineered MSCs expressing P-selectin glycoprotein ligand-1 (PSGL-1) and Sialyl-Lewis^x (SLeX) via mRNA transfection facilitated the targeted delivery of anti-inflammatory cytokine interleukin-10 (IL-10) to inflamed ear. Here, we evaluated whether targeted delivery of MSCs with triple PSGL1/SLeX/IL-10 engineering improves therapeutic outcomes in mouse experimental autoimmune encephalomyelitis (EAE), a murine model for human MS. We found PSGL-1/SLeX mRNA transfection significantly enhanced MSC homing to the inflamed spinal cord. This is consistent with results from *in vitro* flow chamber assays in which PSGL-1/SleX mRNA transfection significantly increased the percentage of rolling and

[*]**Correspondence:** Weian Zhao, weianz@uci.edu University of California, Irvine, 845 Health Sciences Road, Irvine, CA 92697, USA.

Author contributions: W.L, W.Z: Conception and design, Data analysis and interpretation, Manuscript writing; W.L, V.P, M.R and L.L: Collection and/or assembly of data, Data analysis and interpretation; E.P, S.Z, F.M, M.L, X,J and C.W: Data analysis and interpretation, Manuscript writing. W.Z: Supervision of the whole research and final approval of manuscript.

Conflicts of interest:
The authors have no conflicts of interest to declare.

adherent cells on activated brain microvascular endothelial cells, which mimic the inflamed endothelium of blood brain/spinal cord barrier in EAE. In addition, IL-10-transfected MSCs show significant inhibitory activity on the proliferation of $CD4^+$ T lymphocytes from EAE mice. *In vivo* treatment with MSCs engineered with PSGL-1/SLeX/IL-10 in EAE mice exhibited a superior therapeutic function over native (unmodified) MSCs, evidenced by significantly improved myelination and decreased lymphocytes infiltration into the white matter of the spinal cord. Our strategy of targeted delivery of performance-enhanced MSCs could potentially be utilized to increase the effectiveness of MSC-based therapy for MS and other central nervous system (CNS) disorders.

Keywords

Mesenchymal stem cell; MSC, Multiple sclerosis; mRNA transfection; Cell Homing; EAE

Introduction

Multiple sclerosis (MS) is a major cause of neurological disability, an incurable and debilitating disease affecting over 300,000 people in the US[1]. The inefficiency and adverse effects such as severe infections caused by current immunosuppressive agents suggest an unmet need of therapies for MS[2]. Recent evidence has shown that stem cell therapy might offer therapeutic potential for CNS inflammatory diseases including MS[3, 4]. Mesenchymal stem cells (MSCs) are one of the most promising stem cell types for treating MS due to their potent immunomodulatory abilities[2, 5, 6]. There are approximately 21 clinical trials evaluating the MSC treatment for different subtypes of multiple sclerosis (September 2015, Keywords: “Mesenchymal stem cell” AND “Multiple sclerosis”, www.ClinicalTrials.gov). Results from a recent Phase II clinical trial suggested that bone marrow MSCs are safe and may reduce inflammatory parameters (gadolinium-enhancing lesions) measured by magnetic resonance imaging (MRI), in agreement with their immunomodulatory properties in relapsing-remitting MS[7]. However, these clinical trials, overall, have produced mixed results, often documenting the failure of MSC therapies to ameliorate MS. The inconsistent results from different trials are attributed not only to the different MSC sources and preparation (e.g., culture conditions, heterogeneity, passage numbers and genetic modification), but also to the low efficiency of cell delivery to targeted sites and to a lack of control over the cell fate, especially the production of therapeutic and anti-inflammatory factors following transplantation. Thus, overcoming these major bottlenecks would be critical for increasing the efficacy of stem cell based therapy.

Systemic infusion is considered as the most favorable modality for MSC transplantation because of its convenience and minimal invasiveness. Indeed, the majority of both preclinical and clinical studies use systemic infusion for cell delivery[8–10]. Although MSCs have inherent tropism to pathological sites such as inflamed tissue, ischemic tissue and tumors[11–13], mounting evidence suggests that MSC homing is inefficient due partly to the lack of several key professional homing ligands found in the leukocyte homing cascade[14]. There are three main steps during leukocyte homing: tethering/rolling, firm adhesion/arrest, and extravascular transmigration[15, 16]. MSCs express several adhesion molecules including

very late antigen-4 (VLA-4, α4β1 integrin) and vascular cell adhesion molecule-1 (VCAM-1)[17, 18], which are involved in firm adhesion of MSCs on endothelial cells[17, 19]. MSCs have also been shown to efficiently transmigrate through activated endothelial cells via both transcellular and paracellular pathways[19–23]. However, MSCs do not robustly express endothelial P- and E-selectin ligands, including notably P-selectin glycoprotein ligand-1 (PSGL-1) and Sialyl-Lewis^x (SLeX), that are required for tethering and rolling, a critical first step for trafficking cells to adhere on endothelium from the blood stream[17]. Therefore, expression of selectin ligands on MSCs might help increase their trafficking to targeted tissues and the efficiency of drug delivery by MSCs for therapeutic purposes. Indeed, previous studies have shown that engineering MSCs with key cell rolling ligands including hematopoietic cell E-/L-selectin ligand (HCELL) and SLeX led to enhanced homing efficiency to inflammatory and diseased sites[24, 25].

The therapeutic functions of MSCs for autoimmune diseases largely rely on their unique ability to secrete immunomodulatory cytokines[26]. However, the immunomodulatory secretome of MSCs is highly variable, likely due to their active interaction with the components of innate and adaptive immune system and their plasticity and heterogeneity with respect to immunomodulatory function[27]. The uncertainty and lack of control over the *in vivo* MSC secretome present great challenges in achieving predictable and reproducible therapeutic efficacy of MSCs following systemic infusion. Therefore, engineering MSCs with defined immunomodulatory cytokines might maximize their therapeutic utility.

Based on this premise, we have recently demonstrated that systemic administration of MSCs engineered with PSGL-1/SLeX by mRNA transfection improved MSC homing and targeted delivery of the anti-inflammatory cytokine IL-10 in a murine ear inflammation model[25, 28]. mRNA-based protein expression is particularly attractive for such cell engineering due to its simplicity, transient and rapid protein translation after transfection, and ease for expressing multiple factors simultaneously[28–30]. Here, we aimed to examine if such targeted therapeutic delivery can improve the therapeutic efficacy of transplanted stem cells in a clinically relevant setting of CNS inflammatory autoimmune disease. Specifically, we hypothesized that these modified MSCs could home more efficiently to inflamed CNS tissues and increase therapeutic efficacy in mice with experimental autoimmune encephalomyelitis (EAE), a murine model of clinical MS (Figure 1). We found enhanced localization of engineered MSCs in the inflamed spinal cord, the main affected CNS tissue in EAE mice[31], and the engineered MSCs showed superior therapeutic functions over unmodified MSCs. Our results provide a promising strategy for targeted delivery of performance-enhanced MSCs for the treatment of MS and other immune-mediated CNS disorders. In a broader context, our simple mRNA engineering technology may also serve as a platform for engineering and controlling the fate of other types of cells after systemic administration to effectively treat a wide range of diseases.

Materials and Methods

Animals

The usage of animals was in accordance with National Institutes of Health (NIH) guidelines and approved under the Institutional Animal Care and Use Committees (IACUC) of

University of California, Irvine. C57BL/6 (Charles River Laboratories, San Diego, CA) mice were used in all *in vivo* studies.

Cell culture

The primary bone marrow derived MSCs were purchased from Texas A&M Institute of Regenerative Medicine, where these stem cells were characterized and isolated from the healthy bone marrows of consenting donors. CD4+ T cells were isolated from the spleen of C57BL/6 mice spleen. HL-60 cells and brain microvascular endothelial cells (BMECs) were obtained from American Type Culture Collection (ATCC). MSCs were cultured in α-MEM media (Gibco, Life Technology) supplemented with 15% FBS, 1% L-Glutamine and 1% Penicillin-Streptomycin. The HL-60 cells were grown in IMBM medium (Lonza) that has supplements of 20% FBS, 1% L-Glutamine and 1% Penicillin-Streptomycin. BMECs were expanded in endothelial cell medium (Lonza) supplemented with Endothelial Cell Medium Supplement Kit (CellBiologics). All the cultures were incubated at 37°C with 5% CO_2, and the media was changed every two to three days. MSCs at passage 3–6 were used for all experiments.

mRNA synthesis and transfection

All PSGL-1, FUT-7 and IL-10 mRNAs were synthesized as previously described[28] by Factor Bioscience (Boston, MA). Briefly, the *in vitro* transcription of pre-mRNA templates for PSGL-1, FUT-7, and IL-10 have been constructed to all have T7 promoter at the 5' ends and an optimized Kozak sequence in the sequence between the 5' UTR and the start codon. For each pre-mRNA, the protein coding sequence was flanked by the 5' and 3'-untranslated region (UTRs) of the human beta-globin (HBB). This pre-mRNA was synthesized with 5'-cap and 3'-polyadenylate tail using the T7 mScript Standard mRNA Production System protocol kit (CellScript). A modified nucleoside 59-triphosphate solution was used, in which pseudouridine-59-triphosphate (pseudo-UTP) and 5-methylcytidine-59-triphosphate (5-methyl-CTP) were substituted for UTP and CTP, respectively. After transcription, uncapped RNA was purified using an RNeasy kit (Qiagen, Hilden, Germany) and a 59 cap structure and 39-poly(A) tail were added using the T7 mScript kit. For mRNA transfection, PSGL-1, FUT-7, or IL-10 mRNAs (1μg/10cm^2 surface area) were diluted in of Opti-MEM (50 μl/μg mRNA; Gibco, Life Technology). Lipofectamine RNAiMAX (4μ/μg, Invitrogen, Life Technology) were added to the same amount of Opti-MEM and incubated for 5 minutes at room temperature. Then the Lipofectamine and mRNA solution were mixed and incubated for 15 minutes at room temperature before added to MSC culture (serum-free media). Media were changed at 4 hours after the transfection.

Immunostaining and ELISA

MSCs or frozen spinal cord sections were fixed in 4% PFA for 15–30 minutes and 10% goat serum were used to block non-specific binding. Then anti-CD15s (1:100, BioLegend), anti-PSGL-1 (1:100, BioLegend), CD45 (1:100 Tonbo Biosciences) were added and incubated at 4°C overnight. Alexa-488 conjugated Anti-rabbit secondary antibody (Abcam) were then added and incubated for 1 hour at room temperature. The MSCs or tissue sections were then covered by a glass coverslip with DPX mounting solution and analyzed under a fluorescent

microscope. IgG-FITC, and IgM-FITC were used as isotype controls. To quantify the percentage of CD15s or PSGL-1 positive MSCs in the culture dishes, at least 5 random fields from images (20×) taken under fluorescent microscope were analyzed by imageJ and the percentage was calculated as the number of CD15s or PSGL-1 positive cells (green) divided by the total number of cells in the field as indentified by DAPI stained blue nuclei. For the detection of IL-10 secretion, the condition media from either native MSCs or engineered MSCs were collected and analyzed via Human IL-10 ELISA Kit II (BD OptEIA).

In vitro cell rolling and adhesion on BMECs

The BMECs were grown in 6-cm culture dishes until 100% confluent. To mimic inflamed condition, BMECs were activated with TNFα (50ng/mL) for 6 hours before the experiment. PicoPlus syringe pump (Havard Apparatus) and Vacuum pump (Welch) were used for the flow chamber assay to conduct the cell rolling experiments. The flow rates were adjusted according to the desired shear stresses: 4.42 μL/min (1 dyn/cm^2), 8.84 μL/min (2 dyn/cm^2), 17.68 μL/min (5 dyn/cm^2), and 35.36 μL/min (10 dyn/cm^2). The cell rolling and adhesion activities of the engineered MSCs, native MSCs and HL-60 (1×10^5 cells/run) on BMECs monolayers were observed and recorded for further quantification analysis. At least six random 10-second frames from each video were analyzed. ImageJ (Plugin: Stack, manual tracking) was used to quantify the velocity and percentage of the rolling cells. The percentage of rolling cells was calculated as the total number of rolling cells divided by the total number of cells that were injected for those 10 second time frame. At the end of each flow chamber run, images of adherent cells (pre-labeled with DiI or DiO) on BMECs were photographed using build-in Nikon cameras in fluorescent microscope, the number of adherent cells were counted by ImageJ software for statistical analyses.

Co-culture of MSCs and CD4$^+$ T cells

MSCs were engineered 1–2 days prior to co-culturing with CD4+ T-cells. The proliferation of T cells were measured using carboxyfluorescein diacetate succinimidyl ester (CFSE) assay. Briefly, splenocytes were obtained from the EAE mice spleen, after removing red blood cells using ACK lysing buffer (Gibco, Life Technology), EasySep Mouse CD4$^+$ T Cell Isolation kit (StemCell Technology) was used to purify CD4+ T-cells from the splenocytes. These isolated CD4$^+$ T-cells (1×10^7 cells/mL) were pre-stained with CFSE (1μM). Then the CD4$^+$ T-cells (1×10^5) were added onto 24-well plates with confluent engineered MSCs in the presence of anti-CD3 (1ng/μL), anti-CD28 (1ng/μL) antibodies and IL-2 (2ng/μL) in RPMI-1640 medium (Calsson) supplemented with 10% deactivated FBS, 2-mercaptoethanol (50nM), and 1% penicillin and streptomycin. 6 days later, the cultured T cells were harvested and stained with anti-CD4 antibody (1μg/ml) and 7ADD (1μg/ml) before analyzed by flow cytometer.

EAE induction

To induce EAE in mice, complete Freund's adjuvants (CFA) was prepared by mixing *Mycobacterium tuberculosis* (2mg/ml) with Freund's adjuvants (Sigma). An equal amount of MOG$^{35–55}$ peptide (Anaspec Inc., Fremont, CA) (2 mg/mL in ddH_2O) and CFA solution

were mixed to have a final concentration of 1 mg/mL before injected into each mouse. 100 μl of antigen/CFA emulsion was delivered to two different sites of each hind flank, and immediately after that, 400 ng of pertussis toxin were intraperitoneally injected. Another pertussis toxin was given two days later. Clinical signs of EAE disease severity was scored according to the previously described 0–4 scale[32] as follows: 0, no clinical signs; 0.5, tail weakness; 1, completely limp tail; 1.5, limp tail and hindlimb weakness; 2, unilateral hindlimb paralysis; 2.5, bilateral partial hindlimb paralysis; 3, bilateral hindlimb paralysis; 3.5, complete hindlimb and unilateral forelimb paralysis; and 4, death or moribund.

Cell transplantation and homing Assay

EAE mice in engineered MSCs (n=7), native MSCs (n=6) or PBS (n=6) groups received 1 million cells (in 200μl PBS) or PBS only via tail vein injection on day 14 post immunization and clinical scores were evaluated for 21 days after injection. For homing assay, dissociated engineered MSCs or native MSCs were labeled with lipophilic fluorescent dyes (DiD or DiI, 5μg/mL, Invitrogen) before transplantation on day 14 post immunization. Each mouse received a single dose of about 1 million (in 200μl PBS) fluorescently labeled MSCs. For cotransplantation, engineered MSCs and native MSCs were mixed at 1:1 ratio and each animal received a total of 1.5×10^6 cells. PBS injection served as sham control. Mice were sacrificed at 6 hours or 24 hours after injection and frozen sections of spinal cord were analyzed under fluorescent microscope. Cell quantification was performed on at least five spinal cord cross-sections per animal for at least three animals. Homing efficiency was calculated by dividing the estimated total number of homing MSCs in the entire spinal cord by the total number of injected cells.

In vivo tracking of MSCs labeled by luciferase lentivirus

The fluc lentivirus was packaged in 293FT cells by co-transfection of pLenti-fluc-RFP plasmid (2μg), pMDLg/pRRE, pRSV/REV, and pMD2.G using Lipofectamine® LTX (Sigma). The lentivirus containing supernatant were added to MSCs culture and incubated for 24 hours. After the incubation, the media containing the lentiviral particles were removed and new media with puromycin (1 μg/mL) were added to select the successfully transduced cells. A single dose of 1×10^6 cells were injected into EAE mice via tail vein on day 14 post immunization. IVIS Imaging of the mice was observed at 6 hours, and 24 hours after MSCs injection.

Demyelination and inflammation area quantification

Twenty one days after cell injection, mice were sacrificed and spinal cord sections (10μm) were sliced from the block and embedded on a glass slide to be analyzed with luxol fast blue (LFB) staining. 0.1% LFB working solution was made by disolving1 mg LFB powder with 95% ethanol and acetic acid. The spinal cord sections were incubated in the LFB solution for 4 hours at 60°C. Then the excess stain will be differentiated with 0.01% Lithium carbonate in 95% ethanol. Paramount was used to cover the tissues with a glass coverslip. The quantification of demyelination was performed on at least five spinal cord cross-sections per animal. The area of demyelination, each spinal cord section and the grey matter were traced and measured using ImageJ. White matter areas were determined by subtracting the grey matter area from the whole spinal cord area. The same method was applied to

quantify the inflammation area that was identified by CD45+ staining in spinal cord sections as mentioned above.

Statistical analysis

The results are presented as mean ± standard deviation (SD). Experimental and control groups were compare d using an unpaired two-tailed Student's *t*-test. Differences between three or more groups were evaluated by the one-way ANOVA with Dunnett's multiple comparison test. $P < 0.05$ was considered statistically significant.

Results

MSCs transfected with PSGL-1/SLeX exhibit superior rolling and adhesion on inflamed endothelium *in vitro*

P- and E-selectins mediate cell tethering and rolling, a crucial step required to trigger the ensuing firm adhesion of leukocytes on activated endothelial cells and eventually leading to their extravasation to parenchyma of an inflammatory site[16]. Selectin ligands are SLeX–like carbohydrate-containing molecules biosynthesized by glycosyltransferases including α-(1,3)-fucosyltransferase (FUT7)[16, 33]. To bind selectins effectively, the carbohydrate ligand structures must be presented on specialized glycoprotein scaffolds including PSGL-1[16]. PSGL-1/SLeX was used in the current and our previous studies[25, 28] because their interaction with selectins accounts for more than 90% of all the rolling function for T cells[34–36].

While numerous approaches including genetic, enzymatic and chemical modification were used to engineer cells to express homing ligands[24, 25, 37–39], we chose mRNA transfection because of its simplicity in the simultaneous engineering of cells with multiple factors and the rapid and transient expression of proteins to target therapeutic mechanisms that occur rapidly and transiently following cell transplantation therefore avoiding potential long-term safety issues[29, 30]. In particular, recent advances to increase mRNA translational efficiency and stability, and to decrease immunogenicity by cap modifications modified nucleotides[40, 41], further broaden their applications[42–45]. Previously, we showed rapid (maximal expression is typically reached in 1–2 days) and transient (up to 7 days) expression of PSGL-1/SLeX in MSCs transfected with the PSGL-1/FUT-7 mRNAs[28]. In the present study, we confirmed this efficient mRNA transfection using immunostaining for PSGL-1/SLeX 24 hours after mRNA transfection (right before the cell transplantation). As shown in Figure 2A, more than 90% of transfected MSCs expressed PSGL-1 or SLeX, with no detectable expression of either of them in non-transfected MSCs, which is consistent with our previous flow cytometry data[28].

To mimic the dynamics of the rolling and adhesion of systemically infused MSCs on inflamed endothelium, monolayer BMECs were activated with TNF-α to upregulate selectins and firm adhesion molecules[46]. MSC rolling and adhesion on activated BMEC were examined using a conventional parallel flow chamber assay (Figure 2B,C) under shear stresses (1–5dyn/cm^2) relevant to the hydrodynamic conditions found in CNS venules[17, 22]. Previously, we demonstrated that both PSGL-1 and SLeX are required to generate a rolling

response and triple transfections of PSGL-1/SLeX/IL-10 exhibited similar robust rolling behavior as PSGL-1/SLeX transfected MSCs, suggesting that transfection of IL-10 does not affect the adhesive properties of PSGL-1/SLeX[28]. Moreover, we have shown that transfection of IL-10 alone does not display any improved rolling response[28]. Compared to unmodified MSCs that only exhibited a minimal level of cell rolling and adhesion on activated BMEC, MSCs transfected with PSGL-1/SleX had demonstrated a significantly increased frequency of rolling cells (Figure 2D) and decreased cell rolling velocity (Figure 2C,E; Video S1). The overall cell rolling performance of PSGL-1/SleX-engineered MSCs is comparable to (although slightly less robust than) that of HL-60 cells, a promyelocytic leukemia cell line that is commonly used as a positive control for leukocyte rolling. We next demonstrated that significantly more PSGL-1/SLeX-transfected MSCs adhered onto the BMECs as compared with unmodified MSCs under different shear stresses (Figure 3A, B). Similarly, when PSGL-1/SLeX-transfected MSCs and unmodified MSCs labeled with different colored fluorescent dyes were mixed in a 1:1 ratio and run simultaneously in the same flow chamber, significantly higher numbers of transfected MSCs were arrested on activated endothelial monolayers when compared to unmodified MSCs (Figure 3C, D). Collectively, this set of data validates our hypothesis that engineering MSCs with cell rolling selectin ligands is crucial to initiate cell rolling and the downstream firm adhesion cascade.

Enhanced homing of PSGL-1/SLeX-engineered MSCs to spinal cord of EAE mice

We next determined if PSGL-1/SLeX-engineering of MSCs also enable them to home more efficiently to the inflamed CNS tissues in EAE mice. For most of our studies, we focused on examining spinal cord because inflammatory cells predominantly infiltrate the spinal cord with a relative lack of inflammation in the brain in EAE mice model[31]. Initially, we labeled the MSCs with firefly luciferase to monitor the distribution of MSCs in live animals or *ex vivo* CNS organs. However, we were unable to detect any signals at either 6 or 24 hours after transplantation (Figure S1). This is likely due to the limited sensitivity of the luciferase signal and limited total number of MSCs that homed to the CNS. Therefore, we used fluorescent DiD dyes for imaging the spinal cord *ex vivo*. The results showed that the signals in the engineered MSCs group were significantly higher than those in the unmodified MSCs group (Figure 4A, B).

We further compared the homing efficiency of native and PSGL-1/SLeX engineered MSCs by quantification of the cells in spinal cord frozen sections in both wild type (WT) and EAE mice. In one experiment, the native and PSGL-1/SLeX engineered MSCs were labeled with the same fluorescent dye DiD and injected to different individuals of animals. Alternatively, native MSCs and engineered MSCs labeled with different dyes (DiD and DiI, no visible dye transfer between the two labeled MSCs; Figure S2A) were mixed in a 1:1 ratio and injected into mice to compare their competitive homing *in vivo*. We found that unmodified MSCs homed to the spinal cords of EAE mice slightly more efficiently than to WT mice (~1.4% vs. ~1%), although the efficiencies were rather low in both cases (Table S1). This finding is consistent to previous studies that MSCs possess limited homing capability to sites of inflammation[28, 47]. By contrast, PSGL-1/SLeX engineering significantly increased homing efficiency of MSCs in both EAE (~7.6%) (Figure 4C–F, Figure S2B, C, TableS1) and WT

mice (~1.7%) (Table S1, Figure S3). Importantly, this increase was higher in the EAE mice than control mice (Table S1, Figure S4), suggesting that MSCs equipped with PSGL-1/SLeX homing ligands could interact more effectively with P-/E- selectins for the ensuing adhesion and transmigration into the spinal cord parenchyma in EAE mice. This increase probably also attribute to the upregulated levels of P-/E- selectins in the microvascular compartment of CNS in $MOG^{35–55}$ induced C57BL/6 EAE mice[48]. Consistent with this argument, both engineered and unmodified MSCs are localized in the peripheral white matter of spinal cord (Figure 4C,E and Figure S2B), where the inflammation and demyelination occur in EAE mice[49]. Further analysis showed the localization of both engineered and native MSCs was inside the regions infiltrated with immune cells as identified by the typical CD45 and nuclear staining patterns (Figure 4G). As expected, there were significantly more engineered MSCs than unmodified MSCs in the inflammatory regions. We also observed the attachment of engineered MSCs on the lumen surface (vessel-like structure) in spinal cord (Figure 4G), which will be further investigated in our future studies regarding the molecular mechanisms and kinetics of MSC's rolling, adhesion and transmigration across the blood brain/spinal cord barrier *in vivo*. These data confirm previous reports that native MSCs have an increased tropism towards inflammatory sites[28, 47], and PSGL-1/SLeX expression can dramatically enhance the ability of MSCs to home to the inflamed spinal cord in EAE mice.

IL-10 engineered MSCs exhibit enhanced inhibition of $CD4^+$ T cells proliferation *in vitro*

Next we demonstrate that MSCs transfected with IL-10 mRNA exhibit enhanced inhibitory effects on the *in vitro* proliferation of $CD4^+$ T cells isolated from EAE mice. First, we confirmed the efficient mRNA transfection and IL-10 secretion using an ELISA assay. IL-10 was transiently secreted (>10ng from 10,000 seeded cells) from engineered MSCs for up to 7 days while IL-10 secretion was not detected in the supernatant of unmodified MSCs (Figure 5A). In order to assess the immuno-inhibitory function of IL-10-transfected MSCs, we harvested splenocytes from EAE mice and isolated $CD4^+$ T lymphocytes with magnetic cell sorting. $CD4^+$ T cells are thought to be the one of the main effector T cells mediating the pathology of EAE mice[50, 51]. After labeling with CFSE and stimulating them with anti-CD3 and anti-CD28 antibodies and IL-2, $CD4^+$ T cells were co-cultured with recombinant IL-10, native-MSCs or IL-10-engineered MSCs for 6 days and their proliferation was analyzed using flow cytometry. As shown in Figure 5B, IL-10-engineered MSC exhibited significantly enhanced suppression of T-cell proliferation compared to native MSCs and recombinant IL-10.

PSGL-1/SLeX/IL-10 engineered MSCs enhance the neurological recovery of EAE mice

We have previously shown that triple PSGL-1/SleX/IL-10 transfections were required for MSCs engineering to significantly decrease the thickness of LPS-induced inflammatory ear in mouse, while either PSGL/SleX or IL-10 transfection alone failed to enhance the anti-inflammatory effects of MSCs[28]. Based on these important observations, in the current study we determined whether triple PSGL-1/SleX/IL-10 engineered MSCs ameliorates EAE more effectively than control unmodified MSCs, MSCs with or without PSGL-1/SleX/IL-10 engineering (10^6 cells in 200 μl PBS per mouse) were injected via the tail vein at the acute stage of the disease (day 14 post immunization). EAE mice that received the same amount

of PBS served as sham injection controls. As shown in Figure 6A (Video S2), sham-treated mice developed typical EAE, with a mean clinical score of 2.8±0.7 at day 21 post treatment. While unmodified MSC treatment resulted in recovery of neurological function by clinical scoring (mean clinical score: 2.0±0.5), PSGL-1/SLeX/IL-10-engineered MSC treatment elicited a significantly more profound functional improvement (mean clinical score: 1.3±0.6) in the EAE mice.

PSGL-1/SLeX/IL-10 engineered MSCs inhibit demyelination and leukocyte infiltration *in vivo*

As a first step towards understanding the mechanism of how engineered MSCs accelerate functional recovery in mice during EAE, we analyzed the demyelination and inflammatory status of these mice. Demyelination, which leads to neurological deficits, is hallmark of murine EAE and human MS. To compare EAE induced spinal cord demyelination between mice bearing PSGL-1/SLeX/IL10 MSCs, unmodified MSCs (or PBS control groups), the same regions of lumbar spinal cords in the ventral column at L3 were examined at the end of the experiment (21 days post transplantation). Consistent with clinical observations, PBS-treated animals undergoing EAE showed multiple large demyelination areas in the white matter, with an average of about 21% of the white matter demonstrating demyelination. The demyelination was less severe in the spinal cords of EAE mice receiving unmodified MSCs, in which the percentage of demyelination was decreased to ~14%. The percentage of demyelination was further decreased to 6% in spinal cords of EAE mice receiving PSGL-1/SLeX/IL-10-engineered MSCs (Figure 6B, D). In parallel to the demyelination results, the infiltration of $CD45^+$ leukocytes (associated with inflammation) in spinal cords was significantly suppressed by PSGL-1/SLeX/IL-10-engineered MSCs compared to unmodified MSCs and PBS-treated EAE mice at 21 days post transplantation (Figure 6C, E). Notably, the inflammatory regions were generally co-localized with the demyelinated areas in the peripheral white matter of spinal cord[49] (Figure 6B, C). These data suggest a superior anti-inflammatory effect of PSGL-1/SLeX/IL-10-engineered MSCs over unmodified MSCs in EAE animals.

Discussion

MSC-based therapy shows great promise for the treatment of conditions with a predominantly inflammatory/autoimmune component, such as MS[2, 4]. However, it remains difficult to deliver sufficient numbers of stem cells to the site of interest by systemic infusion, which is even more challenging for CNS targeting because of the existence of the blood brain/spinal cord barrier[22]. While it remains controversial whether MSCs are able to transmigrate across the endothelium via leukocyte-like extravasation mechanisms including rolling, adhesion and transmigration, it is clear that the cumulative homing efficiency is rather low[14]. This may be due to the lack of expression of essential homing molecules, especially those involved in cell rolling, including PSGL-1, Mac-1 and LFA-1 on MSCs[17, 52, 53]. In the present study, we demonstrated that engineered expression of PSGL-1/SLeX on MSCs significantly increased their homing to the inflamed CNS parenchyma in EAE mice compared to that of native MSCs. This is consistent with the results of our *in vitro* flow chamber assay, in which few unmodified MSCs were able to build up firm

adhesion onto inflamed BMECs, but more MSCs adhered upon transfection with PSGL-1/SLeX. The absence of the rolling molecules PSGL-1/SLeX in unmodified MSCs may also result in the limited activation of adhesion molecules (integrins) on these cells that are normally required for efficient adhesion and subsequent transmigration. Notably, we observed only slight increases in adherence of modified MSCs on non-inflamed BMECs (i.e., without TNF-α pretreatment) after PSGL-1/SLeX transfection (data not shown). This further confirmed that MSC-expressed PSGL-1/SLeX must interact with P- and/or E-selectin, and these interactions are responsible for the arrest of MSCs on BMECs. Our findings are also consistent with our previous report in which PSGL-1/SLeX mRNA transfection significantly promoted the homing of MSCs to inflamed murine ear[25, 28]. Future efforts are still needed to follow in more detail the kinetics and stages of MSCs extravasation in spinal cord, e.g., by using intravital 2-photon microscopy.

The increased vascular permeability during pathological conditions is generally thought to be an important factor in facilitating stem cell homing to the injured tissues[14, 22]. However, a recent study found that the frequency of MSCs transmigrating across endothelium was unchanged even after increasing the endothelial permeability[23]. In contrast, the absence of P- /E- selectins or their ligand PSGL-1 significantly decreased the recruitment of leukocytes to the CNS microvasculature. The TNF-α induced recruitment of leukocytes to the brain was reduced after treatment with either anti–E- or anti–P-selectin antibody, and this was virtually eliminated in E- or P-selectin–deficient mice[46, 54]. Likewise, anti-P-selectin blocking antibodies prevented nearly all leukocyte rolling and reduced adhesion by about 70% in brain postcapillary venules of EAE mice[55]. Thus, these data suggest that PSGL-1/SLeX interactions with selectins are essential for leukocyte recruitment into CNS tissue upon inflammation. Our data that PSGL-1/SLeX-engineered MSCs in the EAE setting exhibited significantly enhanced homing compared to PSGL-1/SLeX MSCs in WT mice, and native MSCs in WT and EAE mice (Table S1, Figure S4), further demonstrates that engineered MSCs utilize leukocyte-like active homing mechanisms (rolling, adhesion and transmigration) rather than passive capture for the extravasation, even at sites of “leaky” endothelia in inflamed tissues. Therefore, manipulation of leukocyte-like extravasation mechanisms on MSCs may be an effective strategy to facilitate targeted MSC delivery. Future work will exploit combined engineering of both PSGL-1/SLeX and chemokine receptors (e.g., CXCR4 and CCR1) on MSCs that may synergistically promote the homing and extravasation of MSCs to inflamed parenchymal tissues[38, 39, 56].

In the context of inflammatory diseases, the therapeutic functions of MSCs rely largely on their unique ability to secrete immunomodulatory cytokines[26]. Results from most studies have suggested that the recruitment of MSCs into inflamed sites peaks at 24 to 48 hours, and they are usually cleared from the body within one week after systemic infusion[13, 28, 57]. Therefore, it has been hypothesized that MSCs act through a “hit-and-run” mechanism to exert their therapeutic effects[57, 58]. Given the uncertainty and heterogeneity of the MSC secretome after systemic infusion, optimal therapeutic potential can be maximized if MSCs are engineered with controlled production of therapeutic secretome agents (such as IL-10 in current study) and delivered rapidly to targeted sites prior to their death and clearance[28].

Various methods to modify MSCs for the exogenous expression of proteins of interest have been described[25, 38, 39, 59]. In terms of MSC-based therapy, the emerging mRNA transfection technology seems appropriate for increasing MSC homing and their transient delivery of biologic agents. The transfection of mRNA is highly efficient and non-toxic to MSCs when compared to plasmid transfection[30], and it is compatible with ectopic co-expression of multiple mRNAs at the same time. Indeed, previous studies have demonstrated the mRNA transfection-based cell engineering typically has little impact on important cell properties including cell viability and cell differentiation capacity[30, 41]. We have also systematically studied how mRNA transfection process might affect MSC adhesion and rolling on P-selectin coated surface. Using lipofectamine-treated MSCs, as well as MSCs transfected with scrambled RNA or IL-10 alone mRNA, we demonstrated that the mRNA transfection process itself has minimal effect on MSC rolling on P-selectin surface[28]. Also, the risk of insertional mutation when using lentivirus to overexpress a protein is also avoided through the application of transient mRNA transfection. Indeed, the delivery of mRNA is a potential new drug class to deliver genetic information, and several clinical trials are exploring the efficacy of mRNA and other types of regulatory RNAs, as *bona fide* drugs[29]. As MSCs begin to appear in inflamed tissue within 30 minutes after systemic infusion and peak there during the following 24 to 48 hours[23, 28], permanent gene transduction for expression of homing ligands may be unnecessary. In addition, MSCs have been thought to act through a transient “hit-and-run” mode to exert their immunosuppressive functions[28, 57, 60], which is compatible with the transient mRNA transfection used in these and other studies. For instance, in the most common subtype of MS, relapsing-remitting MS (RRMS), engineered MSCs could be injected for transient immunosuppression during the relapse stage without raising unintended consequences of MSCs during the remission stages of the disease. This approach also has the potential to minimize the long-term side effects of agents delivered by MSCs, such as IL-10 in this study, given that they may no longer be needed after treatment. Thus, the process of mRNA-engineering enables rapid and transient induction of protein expression to increase MSC homing, as well as MSC mediated delivery of therapeutic agents to sites of interest.

Our current studies focus on further mechanistic investigations of how MSCs exert therapeutic effects at the inflammation sites including examining the levels of IL-10 and other immunomodulatory factors in vivo, as well as how engineered MSCs interact and regulate the immune cells at single-cell level in the spinal cords of EAE mice. We will also quantitatively compare PSGL-1/SLeX/IL-10-engineered cells with cells engineered with only PSGL-1/SLeX or IL-10 with respect to their roles in therapeutic improvement as our previous study demonstrated that only the triple engineered MSC exhibited the most profound therapeutic effects in the murine ear inflammation model[28].

In conclusion, we demonstrate significantly improved therapeutic outcomes of stem cell therapy via manipulation of cell fate following transplantation, and through targeted homing and controlled secretome, which addresses the major bottleneck of lacking control over cell fate in clinical translation of cell therapy. In addition, engineered cell homing to CNS tissues, as demonstrated in this study, offers new opportunities for using stem cells to deliver therapeutic agents for a variety of CNS injuries and diseases.

Supplementary Material

Refer to Web version on PubMed Central for supplementary material.

Acknowledgement

This work was supported by CIRM fellowship TG2-01152 (W.L), CIRM Bridges to Stem Cell Research Program (V.P); NIH Director's New Innovator Awards (DP2) 1DP2CA195763-01 (W.Z) and American Heart Association 13BGIA17140099 (W.Z).

References

1. Adelman G, Rane SG, Villa KF. The cost burden of multiple sclerosis in the United States: a systematic review of the literature. Journal of medical economics. 16:639–647. [PubMed: 23425293]
2. Uccelli A, Laroni A, Freedman MS. Mesenchymal stem cells as treatment for MS - progress to date. Multiple sclerosis (Houndmills, Basingstoke, England). 19:515–519.
3. Liu SP, Fu RH, Huang SJ, et al. Stem cell applications in regenerative medicine for neurological disorders. Cell transplantation. 22:631–637. [PubMed: 23127757]
4. Ben-Hur T. Cell therapy for multiple sclerosis. Neurotherapeutics. 8:625–642. [PubMed: 21904787]
5. Gharibi T, Ahmadi M, Seyfizadeh N, et al. Immunomodulatory characteristics of mesenchymal stem cells and their role in the treatment of Multiple Sclerosis. Cellular immunology. 293:113–121. [PubMed: 25596473]
6. Eckert MA, Vu Q, Xie K, et al. Evidence for high translational potential of mesenchymal stromal cell therapy to improve recovery from ischemic stroke. J Cereb Blood Flow Metab. 33:1322–1334. [PubMed: 23756689]
7. Llufriu S, Sepulveda M, Blanco Y, et al. Randomized placebo-controlled phase II trial of autologous mesenchymal stem cells in multiple sclerosis. PloS one. 9:e113936. [PubMed: 25436769]
8. Vu Q, Xie K, Eckert M, et al. Meta-analysis of preclinical studies of mesenchymal stromal cells for ischemic stroke. Neurology. 82:1277–1286. [PubMed: 24610327]
9. Peng W, Sun J, Sheng C, et al. Systematic review and meta-analysis of efficacy of mesenchymal stem cells on locomotor recovery in animal models of traumatic brain injury. Stem cell research & therapy. 6:47.
10. Doeppner TR, Hermann DM. Stem cell-based treatments against stroke: observations from human proof-of-concept studies and considerations regarding clinical applicability. Frontiers in cellular neuroscience. 8:357. [PubMed: 25400548]
11. Eseonu OI, De Bari C. Homing of mesenchymal stem cells: mechanistic or stochastic? Implications for targeted delivery in arthritis. Rheumatology (Oxford, England). 54:210–218.
12. Droujinine IA, Eckert MA, Zhao W. To grab the stroma by the horns: from biology to cancer therapy with mesenchymal stem cells. Oncotarget. 4:651–664. [PubMed: 23744479]
13. Kidd S, Spaeth E, Dembinski JL, et al. Direct evidence of mesenchymal stem cell tropism for tumor and wounding microenvironments using in vivo bioluminescent imaging. Stem cells (Dayton, Ohio). 2009; 27:2614–2623.
14. Karp JM, Leng Teo GS. Mesenchymal stem cell homing: the devil is in the details. Cell stem cell. 2009; 4:206–216. [PubMed: 19265660]
15. Masopust D, Schenkel JM. The integration of T cell migration, differentiation and function. Nature reviews. 13:309–320.
16. Ley K, Kansas GS. Selectins in T-cell recruitment to non-lymphoid tissues and sites of inflammation. Nature reviews. 2004; 4:325–335.
17. Ruster B, Gottig S, Ludwig RJ, et al. Mesenchymal stem cells display coordinated rolling and adhesion behavior on endothelial cells. Blood. 2006; 108:3938–3944. [PubMed: 16896152]

18. Segers VF, Van Riet I, Andries LJ, et al. Mesenchymal stem cell adhesion to cardiac microvascular endothelium: activators and mechanisms. American journal of physiology. 2006; 290:H1370–H1377. [PubMed: 16243916]
19. Steingen C, Brenig F, Baumgartner L, et al. Characterization of key mechanisms in transmigration and invasion of mesenchymal stem cells. Journal of molecular and cellular cardiology. 2008; 44:1072–1084. [PubMed: 18462748]
20. Schmidt A, Ladage D, Steingen C, et al. Mesenchymal stem cells transmigrate over the endothelial barrier. European journal of cell biology. 2006; 85:1179–1188. [PubMed: 16824647]
21. Matsushita T, Kibayashi T, Katayama T, et al. Mesenchymal stem cells transmigrate across brain microvascular endothelial cell monolayers through transiently formed inter-endothelial gaps. Neuroscience letters. 502:41–45. [PubMed: 21798315]
22. Liu L, Eckert MA, Riazifar H, et al. From blood to the brain: can systemically transplanted mesenchymal stem cells cross the blood-brain barrier? Stem cells international. 2013:435093. [PubMed: 23997771]
23. Teo GS, Yang Z, Carman CV, et al. Intravital imaging of mesenchymal stem cell trafficking and association with platelets and neutrophils. Stem cells (Dayton, Ohio). 33:265–277.
24. Sackstein R, Merzaban JS, Cain DW, et al. Ex vivo glycan engineering of CD44 programs human multipotent mesenchymal stromal cell trafficking to bone. Nature medicine. 2008; 14:181–187.
25. Sarkar D, Spencer JA, Phillips JA, et al. Engineered cell homing. Blood. 118:e184–e191. [PubMed: 22034631]
26. Sridharan R, Karp JM, Zhao W. Bioengineering tools to elucidate and control the fate of transplanted stem cells. Biochemical Society transactions. 42:679–687. [PubMed: 24849237]
27. Bernardo ME, Fibbe WE. Mesenchymal stromal cells: sensors and switchers of inflammation. Cell stem cell. 13:392–402. [PubMed: 24094322]
28. Levy O, Zhao W, Mortensen LJ, et al. mRNA-engineered mesenchymal stem cells for targeted delivery of interleukin-10 to sites of inflammation. Blood. 122:e23–32. [PubMed: 23980067]
29. Sahin U, Kariko K, Tureci O. mRNA-based therapeutics--developing a new class of drugs. Nat Rev Drug Discov. 13:759–780. [PubMed: 25233993]
30. Wiehe JM, Ponsaerts P, Rojewski MT, et al. mRNA-mediated gene delivery into human progenitor cells promotes highly efficient protein expression. Journal of cellular and molecular medicine. 2007; 11:521–530. [PubMed: 17635643]
31. Pierson E, Simmons SB, Castelli L, et al. Mechanisms regulating regional localization of inflammation during CNS autoimmunity. Immunological reviews. 248:205–215. [PubMed: 22725963]
32. Hermann-Kleiter N, Meisel M, Fresser F, et al. Nuclear orphan receptor NR2F6 directly antagonizes NFAT and RORgammat binding to the Il17a promoter. Journal of autoimmunity. 39:428–440. [PubMed: 22921335]
33. Luster AD, Alon R, von Andrian UH. Immune cell migration in inflammation: present and future therapeutic targets. Nature immunology. 2005; 6:1182–1190. [PubMed: 16369557]
34. Xu H, Manivannan A, Crane I, et al. Critical but divergent roles for CD62L and CD44 in directing blood monocyte trafficking in vivo during inflammation. Blood. 2008; 112:1166–1174. [PubMed: 18391078]
35. Ley K, Bullard DC, Arbones ML, et al. Sequential contribution of L- and P-selectin to leukocyte rolling in vivo. The Journal of experimental medicine. 1995; 181:669–675. [PubMed: 7530761]
36. Varki A. Selectin ligands. Proceedings of the National Academy of Sciences of the United States of America. 1994; 91:7390–7397. [PubMed: 7519775]
37. Guan M, Yao W, Liu R, et al. Directing mesenchymal stem cells to bone to augment bone formation and increase bone mass. Nature medicine. 18:456–462.
38. Huang J, Zhang Z, Guo J, et al. Genetic modification of mesenchymal stem cells overexpressing CCR1 increases cell viability, migration, engraftment, and capillary density in the injured myocardium. Circulation research. 106:1753–1762. [PubMed: 20378860]
39. Yu X, Chen D, Zhang Y, et al. Overexpression of CXCR4 in mesenchymal stem cells promotes migration, neuroprotection and angiogenesis in a rat model of stroke. Journal of the neurological sciences. 316:141–149. [PubMed: 22280945]

40. Kariko K, Buckstein M, Ni H, et al. Suppression of RNA recognition by Toll-like receptors: the impact of nucleoside modification and the evolutionary origin of RNA. Immunity. 2005; 23:165–175. [PubMed: 16111635]
41. Kariko K, Muramatsu H, Welsh FA, et al. Incorporation of pseudouridine into mRNA yields superior nonimmunogenic vector with increased translational capacity and biological stability. Mol Ther. 2008; 16:1833–1840. [PubMed: 18797453]
42. Warren L, Manos PD, Ahfeldt T, et al. Highly efficient reprogramming to pluripotency and directed differentiation of human cells with synthetic modified mRNA. Cell stem cell. 7:618–630. [PubMed: 20888316]
43. Angel M, Yanik MF. Innate immune suppression enables frequent transfection with RNA encoding reprogramming proteins. PloS one. 5:e11756. [PubMed: 20668695]
44. Kormann MS, Hasenpusch G, Aneja MK, et al. Expression of therapeutic proteins after delivery of chemically modified mRNA in mice. Nature biotechnology. 29:154–157.
45. Kariko K, Muramatsu H, Keller JM, et al. Increased erythropoiesis in mice injected with submicrogram quantities of pseudouridine-containing mRNA encoding erythropoietin. Mol Ther. 20:948–953. [PubMed: 22334017]
46. Carvalho-Tavares J, Hickey MJ, Hutchison J, et al. A role for platelets and endothelial selectins in tumor necrosis factor-alpha-induced leukocyte recruitment in the brain microvasculature. Circulation research. 2000; 87:1141–1148. [PubMed: 11110771]
47. Rustad KC, Gurtner GC. Mesenchymal Stem Cells Home to Sites of Injury and Inflammation. Advances in wound care. 1:147–152. [PubMed: 24527296]
48. Alt C, Duvefelt K, Franzen B, et al. Gene and protein expression profiling of the microvascular compartment in experimental autoimmune encephalomyelitis in C57Bl/6 and SJL mice. Brain pathology (Zurich, Switzerland). 2005; 15:1–16.
49. Constantinescu CS, Farooqi N, O'Brien K, et al. Experimental autoimmune encephalomyelitis (EAE) as a model for multiple sclerosis (MS). British journal of pharmacology. 164:1079–1106. [PubMed: 21371012]
50. Fletcher JM, Lalor SJ, Sweeney CM, et al. T cells in multiple sclerosis and experimental autoimmune encephalomyelitis. Clinical and experimental immunology. 162:1–11. [PubMed: 20682002]
51. Sonobe Y, Jin S, Wang J, et al. Chronological changes of CD4(+) and CD8(+) T cell subsets in the experimental autoimmune encephalomyelitis, a mouse model of multiple sclerosis. The Tohoku journal of experimental medicine. 2007; 213:329–339. [PubMed: 18075237]
52. Spaeth E, Klopp A, Dembinski J, et al. Inflammation and tumor microenvironments: defining the migratory itinerary of mesenchymal stem cells. Gene therapy. 2008; 15:730–738. [PubMed: 18401438]
53. da Silva Meirelles L, Caplan AI, Nardi NB. In search of the in vivo identity of mesenchymal stem cells. Stem cells (Dayton, Ohio). 2008; 26:2287–2299.
54. Piccio L, Rossi B, Scarpini E, et al. Molecular mechanisms involved in lymphocyte recruitment in inflamed brain microvessels: critical roles for P-selectin glycoprotein ligand-1 and heterotrimeric G(i)-linked receptors. J Immunol. 2002; 168:1940–1949. [PubMed: 11823530]
55. Kerfoot SM, Kubes P. Overlapping roles of P-selectin and alpha 4 integrin to recruit leukocytes to the central nervous system in experimental autoimmune encephalomyelitis. J Immunol. 2002; 169:1000–1006. [PubMed: 12097407]
56. Cheng Z, Ou L, Zhou X, et al. Targeted migration of mesenchymal stem cells modified with CXCR4 gene to infarcted myocardium improves cardiac performance. Mol Ther. 2008; 16:571–579. [PubMed: 18253156]
57. Lee RH, Pulin AA, Seo MJ, et al. Intravenous hMSCs improve myocardial infarction in mice because cells embolized in lung are activated to secrete the anti-inflammatory protein TSG-6. Cell stem cell. 2009; 5:54–63. [PubMed: 19570514]
58. von Bahr L, Batsis I, Moll G, et al. Analysis of tissues following mesenchymal stromal cell therapy in humans indicates limited long-term engraftment and no ectopic tissue formation. Stem cells (Dayton, Ohio). 30:1575–1578.

59. Stiehler M, Duch M, Mygind T, et al. Optimizing viral and non-viral gene transfer methods for genetic modification of porcine mesenchymal stem cells. Advances in experimental medicine and biology. 2006; 585:31–48. [PubMed: 17120775]

60. Ranganath SH, Levy O, Inamdar MS, et al. Harnessing the mesenchymal stem cell secretome for the treatment of cardiovascular disease. Cell stem cell. 10:244–258. [PubMed: 22385653]

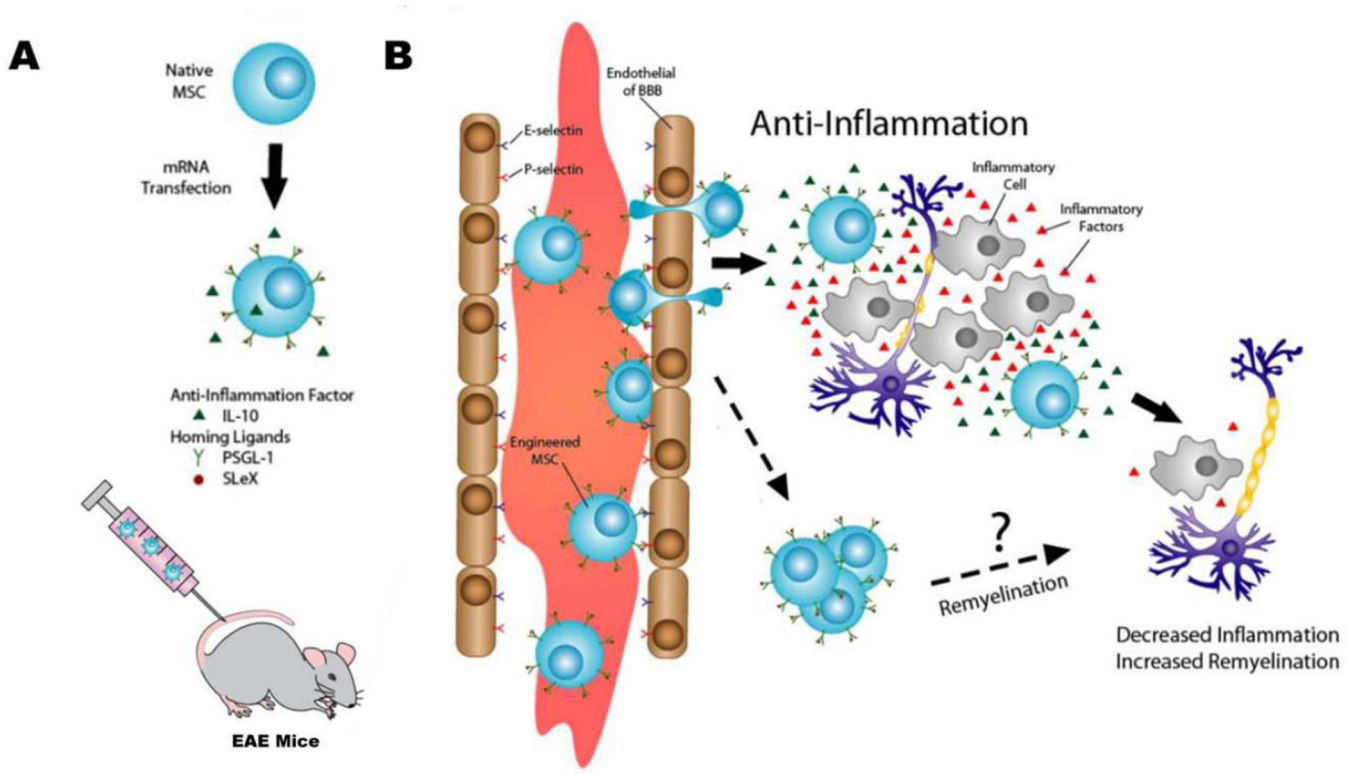

Figure 1.

Illustration of mRNA transfected MSCs with homing ligands and immunomodulatory factors to improve their therapeutic effects in EAE mice. (A) MSCs are engineered to express a combination of homing ligands (PSGL-1 and SLeX) and anti-inflammatory factor (IL-10) via mRNA transfection and infused into EAE mice systemically (tail vein). (B) mRNA-engineered MSCs home to inflamed CNS tissues by crossing blood brain/spinal cord barrier and exert their therapeutic functions by anti-inflammatory and/or other potential remyelination mechanisms.

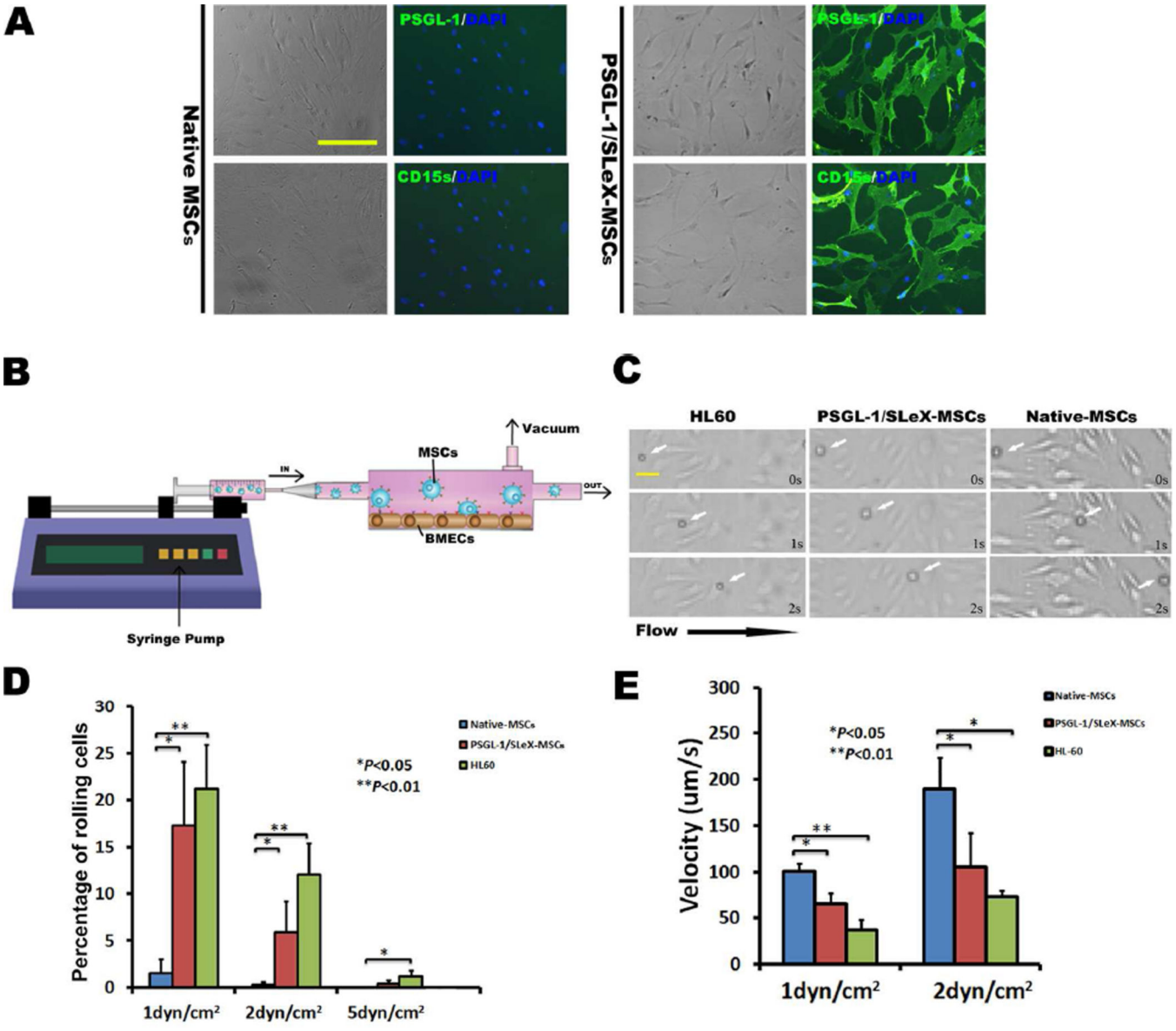

Figure 2.

Enhanced rolling ability of engineered MSCs in a flow chamber assay. (A) The majority of (>90%) mRNA transfected MSCs express PSGL-1 and SLeX as shown by anti-PSGL-1 and anti-CD15s antibody staining, respectively. The native MSCs are negative for either PSGL-1 or SLeX expression. Scale bar=100μm. (B) Illustration of flow chamber assay. (C) Representative images showing PSGL-1/SLeX MSCs (white arrows) roll on TNF-α activated BMECs surface *in vitro* at a comparable velocity as HL-60, while at a substantially lower velocity than native MSCs. Shear stress in these images: 2dyn/cm^2. Scale bar=25μm. (D) Percentage of rolling cells on activated BMECs in PSGL-1/SLeX MSCs, Native MSCs and HL-60 groups. (E) Rolling velocity of PSGL-1/SLeX MSCs, Native MSCs and HL-60 cells on activated BMECs (at least 20 cells were analyzed in each group).

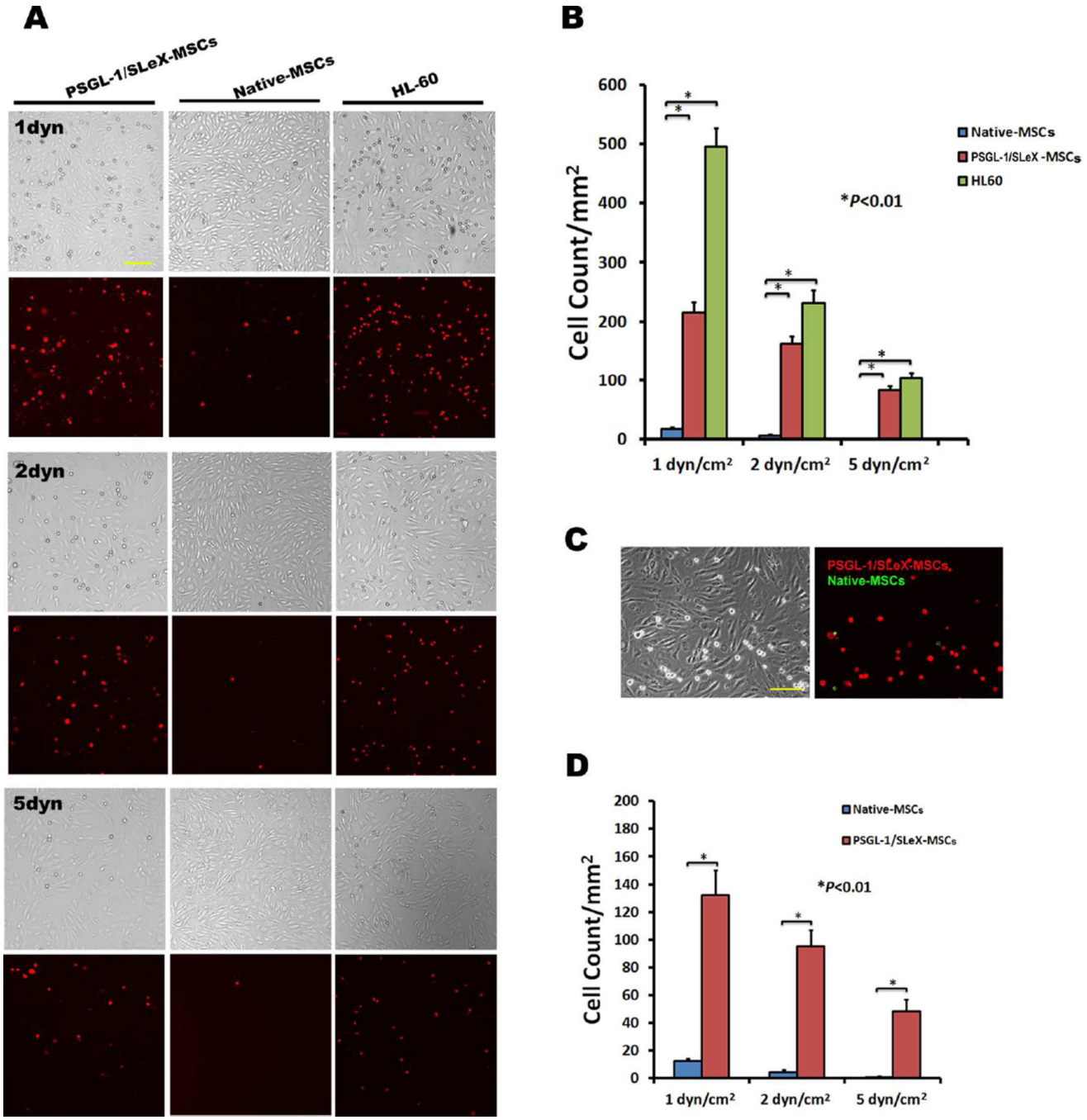

Figure 3.

Increased adhesion of MSCs engineered with PSGL-1/SLeX on activated BMECs under flow conditions. (A) Representative brightfield and fluorescent images demonstrated that significantly more cells (red) adhere on TNF-α activated BMECs in PSGL-1/SLeX MSCs groups than those in native MSCs groups under three different sheer stresses (1, 2 and 5 dyn/cm^2). Scale bar=100μm. This set of experiments is quantified in (B). (C) Representative images of adhered cells in a flow chamber (2 dyn/cm^2) running a mixture of DiI labeled PSGL-1/SLeX MSCs (red) and DiO labeled native MSCs (green) at 1:1 cell ratio. Scale

bars=100μm. A total of 1×10^5 cells were run for each flow chamber assay. This set of experiments is quantified in (D). At least three random areas were selected for cell counting using ImageJ. Data were presented as Mean±SD.

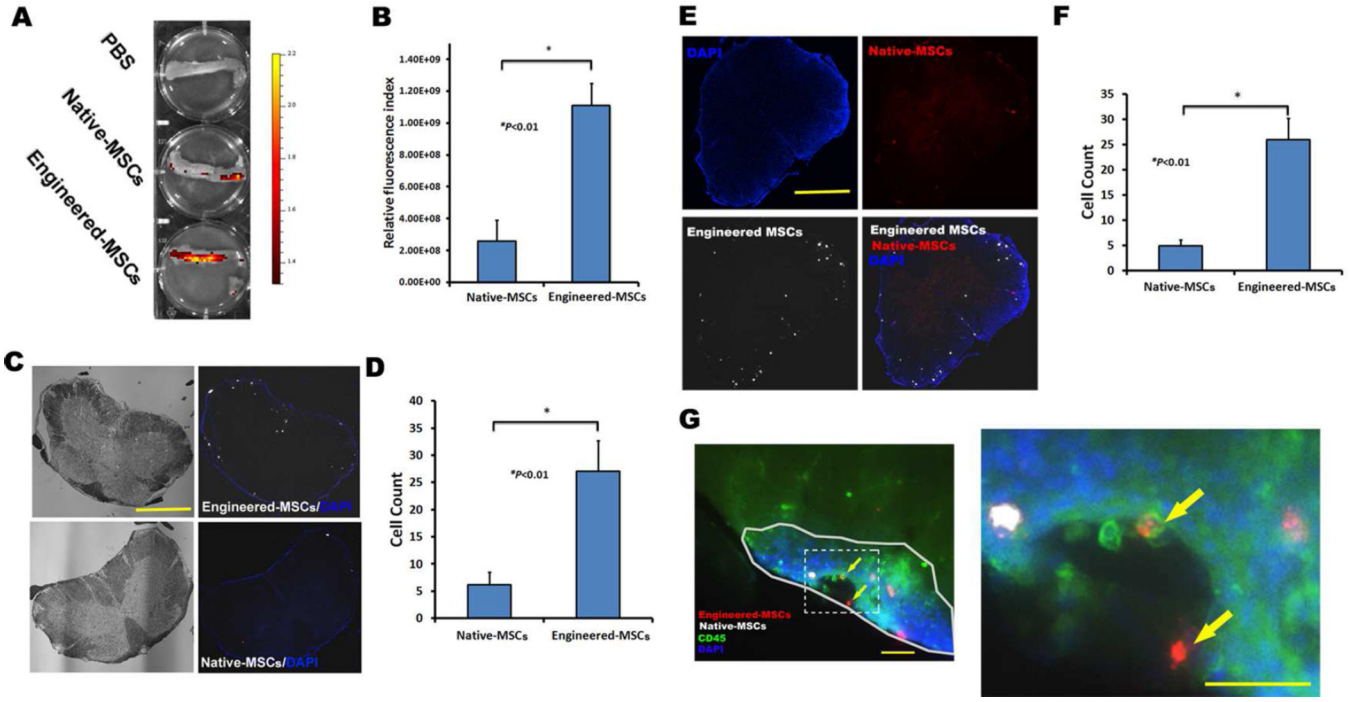

Figure 4.

Increased homing of PSGL-1/SLeX engineered MSCs to spinal cords of EAE mice after systemic administration. (A-B) Representative image and quantification of signals of DID labeled MSCs in spinal cord using IVIS imaging 24 hours after cell transplantation. (C–D) PSGL-1/SLeX engineered MSCs show enhanced homing ability to spinal cords as compared to native MSCs. Scale bar=500μm. (E–F) Injection of a mixture of DiD labeled PSGL-1/SLeX MSCs (white) and DiI labeled native MSCs (red) confirms the superior homing ability of engineered MSCs to EAE spinal cords. Scale bar=500μm. (G) Representative image shows that both engineered MSCs (red) and native MSCs (white) localize in inflammatory region (marked by solid line) as identified by CD45 staining (green) and higher cellular density (blue) in the white matter of EAE spinal cord. Two engineered MSCs (yellow arrows) adhere onto the luminal surface of a blood vessel-like structure. The right image is the magnification of the square box (marked by dash line) of the left image. Scale bars=100 μm.

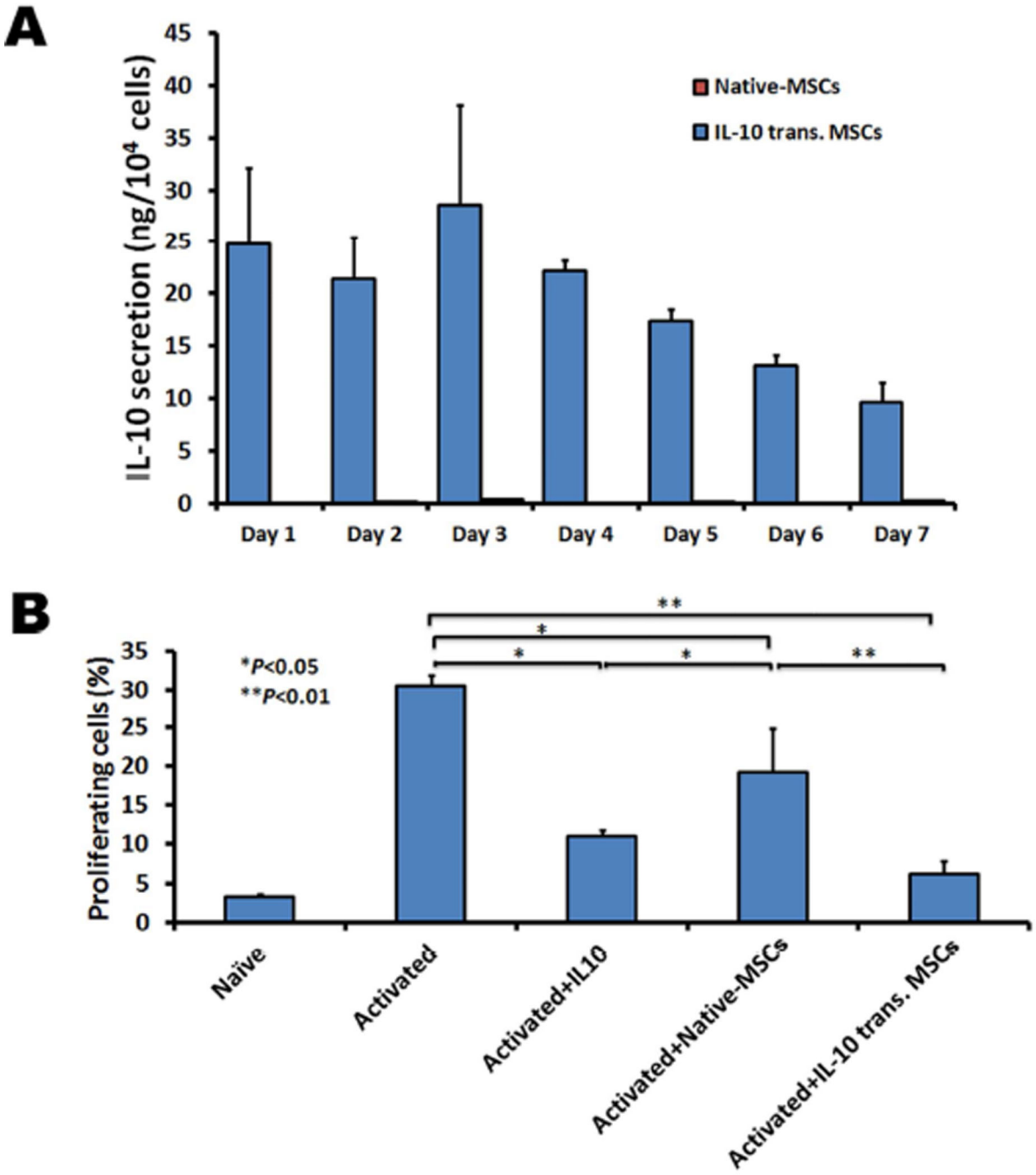

Figure 5.

Inhibitory activity of IL-10 transfected MSCs on T cell proliferation *in vitro*. (A) mRNA transfected MSCs exhibit robust secretion of IL-10 up to seven days (Data bars for native-MSCs are hardly to see due to the low or undetectable IL-10 expression). (B) mRNA transfected MSCs exhibit superior inhibitory effects on CD4+ T cell proliferation isolated from EAE mice spleen as compared to IL-10 or native MSCs. Murine EAE spleen CD4+ T cells were cocultured with native or IL-10-transfected MSCs in the presence of CD3/CD28 monoclonal antibodies and IL-2, and CD4+ T cell proliferation was measured using CFSE

assay (7-AAD staining was used to identify dead cells). Error bars represent standard deviation (SD) (n=3).

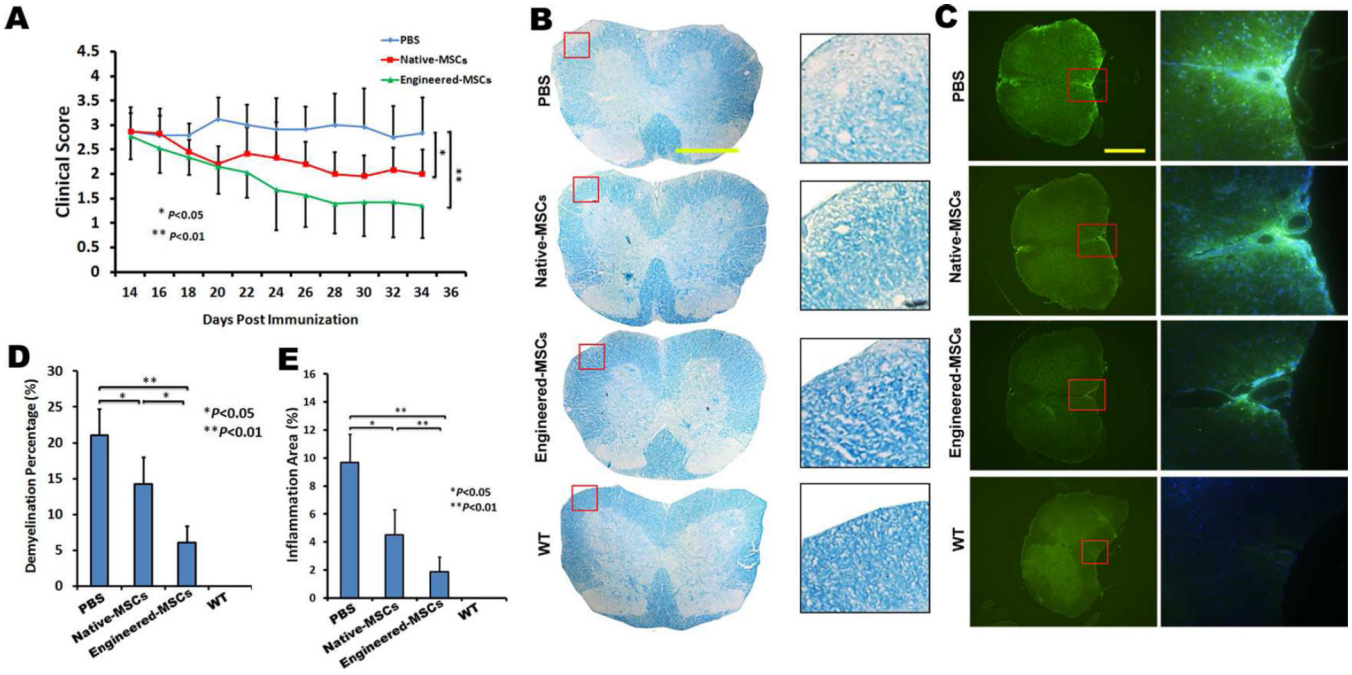

Figure 6.

Triple PSGL-1/SLeX/IL-10 transfected MSCs exhibit improved therapeutic function in EAE mice. (A) Clinical scores show engineered MSCs treatment (n=7) significantly accelerate the functional recovery of EAE mice, as compared to native MSCs (n=6) or PBS (n=6) treated mice. (B) Representative images of demyelination (pale area in white matter) of spinal cords by luxol fast blue (LFB) staining. Scale bar=500μm. (C) Representative images of inflammation of spinal cords by anti-CD45 staining (green). Scale bar=500μm. (D) Quantification of the percentage of demyelination areas in white matter of EAE spinal cords. (E) Quantification of the percentage of inflammation areas (CD45+ staining) in white matter of EAE spinal cords.